Available online at www.sciencedirect.com
ScienceDirect
Composite Structures 82 (2008) 488–498
COMPOSITE STRUCTURES
www.elsevier.com/locate/compstruct

Stress singularities in bimaterial bodies of revolution

C.S. Huang [a,*], A.W. Leissa [b]

[a] Department of Civil Engineering, National Chiao Tung University, 1001 Ta-Hsueh Road, Hsinchu, Taipei 30050, Taiwan
[b] Department of Mechanical Engineering, Colorado State University, Fort Collins, CO 80523, United States

Available online 30 January 2007

Abstract

An eigenfunction expansion solution is first developed for determining the stress singularities of bimaterial bodies of revolution by directly solving the equilibrium equations of three-dimensional elasticity in terms of displacement functions. The characteristic equations are explicitly given for determining the stress singularities in the vicinity of the interface corner of two intersecting bodies of revolution having a sharp corner with free boundary conditions along the corner. The characteristic equations are found to be equivalent to a combination of the characteristic equations for plane elasticity problems and St. Venant torsion problems. The strength of stress singularities varying with the interface angles is also investigated. The first known asymptotic solutions for the displacement and stress fields are also explicitly shown for some interface angles. The present results will be useful not only for understanding the singularity behaviors of stresses in the vicinity of a revolution interface corner, but also for developing accurate numerical solutions with fast convergence for stress or vibration analysis of a body of revolution having an interface corner.

Keywords: Stress singularities; Asymptotic solution; Eigenfunction expansion method; Bimaterial bodies of revolution

1. Introduction

Stress singularities mean that stresses go to infinity at some points of the problem domain under consideration. Although stress singularities cannot be real in a practical problem, because of material limitations, they do yield a useful mathematical model for a practical problem. The stress singularities have to be taken into account if the analysis is to be of real use. Williams [1,2] first showed the stress singularities in the sharp corner of a thin plate under extension or bending with various boundary conditions along the intersecting edges.

It is well known that stress singularity behavior has to be properly considered to have a convergent and accurate numerical solution. The stress singularities have been taken into account in different numerical approaches with various ways. The knowledge of stress singularity orders is found to be very important to have correct r^{λ} type singular elements in a finite element approach for solving a crack problem (i.e. [3]). The asymptotic solutions for the stress singularities were introduced into an element free Galerkin method by Belytschko et al. [4] and Fleming et al. [5] to analyze crack problems of plane elasticity. The asymptotic solutions (also called corner functions) based on thin plate theory and Mindlin plate theory [2,6] were introduced into the Ritz method to obtain very accurate results for the vibrations of cantilevered skew plates [7,8].

Based on three-dimensional elasticity, an extensive amount of research has been carried out for investigating the singular stress field at a crack tip, which is very important to fracture mechanics. Sih [9] provided a comprehensive review on works before 1970 of singular stress at the crack tip. Panasyuk et al. [10,11] reviewed more than 500 papers on the analysis of three-dimensional crack problems. In the last two decades, numerous papers were also published on this topic. For example, Ting [12] provided an explicit solution for the singularities at the interface crack in anisotropic composites, while Barsoum and Chen [13] and Ghahremani and Shih [14] investigated surface singularity of an interface crack via a finite element approach.

* Corresponding author. Tel.: +886 35712121; fax: +886 35716257.
E-mail addresses: cshuang@mail.nctu.edu.tw (C.S. Huang), awleissa@mindspring.com (A.W. Leissa).

0263-8223/$ - see front matter © 2007 Elsevier Ltd. All rights reserved.
doi:10.1016/j.compstruct.2007.01.026

Su and Sun [15] extended Gregory's solution [16] to study singular stress at the crack tip of a thick plate. Chaudhuri and Xie [17] used the eigenfunction expansion method to analyze three-dimensional crack problems of isotropic and homogeneous plates.

Much less research has been conducted for studying the geometrically-induced stress singularities at a three-dimensional vertex, of which a crack problem is a special case. Most of these works were based on numerical approaches. One analysis of the stresses in the vicinity of boundary discontinuities was summarized by Zak [18] for the special case of axisymmetric loading. Aksentian [19] analytically obtained the characteristic equations for determining the stress singularities at the vertex of a bi-material wedge with various combinations of boundary conditions along the radial faces. However, his solution did not consider the boundary conditions on the surface with the normal of the thickness direction. Bažant [20] and Bažant and Estenssoro [21] provided a general numerical method to determine the stress singularities in notched elastic solids. Kerr and Parihar [22] studied the stress singularities at the vertex of pyramidal notches with three equal angles by using a Green's function method. Extending Bažant's approach, Somaratna and Ting [23] and Ghahremani [24] used a finite element approach to investigate stress singularities in anisotropic materials and composites, and Picu and Gupta [25] investigated the stress singularities at the tip of a grain triple junction line intersecting the free surface. Using boundary integral equations, Schmitz et al. [26] and Glushkov et al. [27] computed the singularity field at a vertex and at the top of an arbitrary polyhedral corner, respectively. Koguchi and Takashi [28] applied a boundary element approach to determine the order of stress singularity at the corner where four free surfaces and the interfaces of the three-dimensional joints meet. The asymptotic solution at the vertex cannot be explicitly expressed in these numerical approaches. Recently, Huang and Leissa [29] developed the asymptotic solution for the stress singularities at the vertex of a body of revolution by using the eigenfunction expansion method.

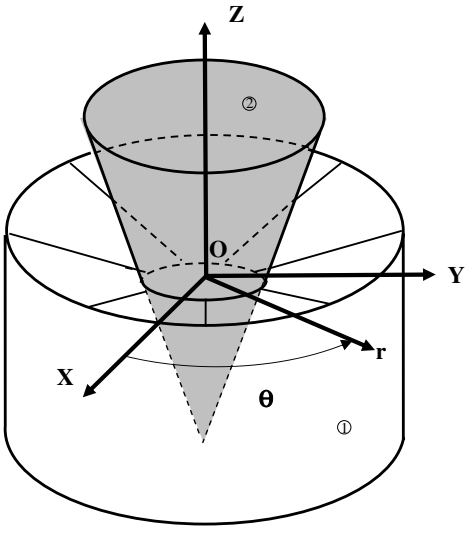

Fig. 1. Bimaterial body of revolution with a sharp corner boundary discontinuity.

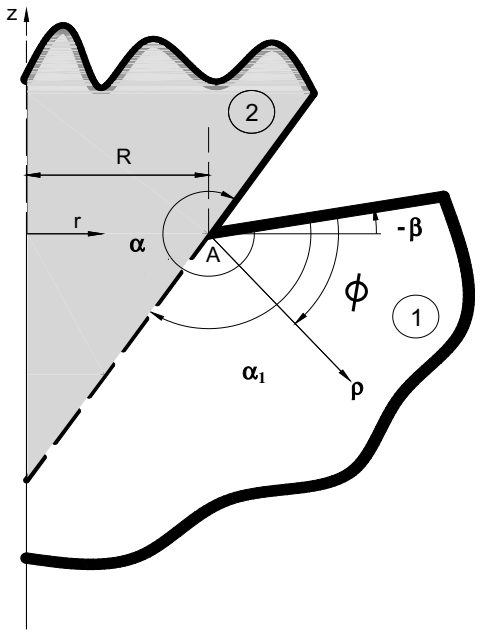

Fig. 2. Cylindrical (r,z) and sharp corner (ρ,ϕ) coordinates.

In the aforementioned studies, none has considered the geometrically-induced stress singularities in bimaterial bodies of revolution based on three-dimensional elasticity. Consequently, this paper extends the authors' previous work [29] to construct the first known asymptotic solutions for the stress singularities along the interface circumference on X–Y plane in Fig. 1, in which bodies of revolution ① and ② have different material properties. The present work uses the eigenfunction expansion method to asymptotically solve the equilibrium equations in terms of displacements of the three-dimensional elasticity theory. The characteristic equations determining the stress singularity order are explicitly given and the effects of material properties and interface angles (α and α_1 in Fig. 2) on the stress singularity orders are also discussed.

2. Analysis

Considering two isotropic and homogeneous bodies of revolution with different elastic materials joined as shown in Fig. 1, each body, subjected to no body forces, should satisfy the following equilibrium equations in terms of displacement components in the cylindrical coordinate system (r,θ,z) (see Fig. 1):

$$2(1-\upsilon_i)u^{(i)}_{,rr}+\frac{2(1-\upsilon_i)}{r}u^{(i)}_{,r}-2(1-\upsilon_i)\frac{u^{(i)}}{r^2}+\frac{1-2\upsilon_i}{r^2}u^{(i)}_{,\theta\theta}+(1-2\upsilon_i)u^{(i)}_{,zz}+\frac{1}{r}v^{(i)}_{,r\theta}-\frac{3-4\upsilon_i}{r^2}v^{(i)}_{,\theta}+w^{(i)}_{,rz}=0, \tag{1a}$$

$$\frac{1}{r}u^{(i)}_{,r\theta}+\frac{3-4\upsilon_i}{r^2}u^{(i)}_{,\theta}+(1-2\upsilon_i)v^{(i)}_{,rr}+(1-2\upsilon_i)\frac{v^{(i)}_{,r}}{r}-(1-2\upsilon_i)\frac{v^{(i)}}{r^2}+\frac{2(1-\upsilon_i)}{r^2}v^{(i)}_{,\theta\theta}+(1-2\upsilon_i)v^{(i)}_{,zz}+\frac{1}{r}w^{(i)}_{,\theta z}=0, \tag{1b}$$

$$u^{(i)}_{,rz}+\frac{u^{(i)}_{,z}}{r}+\frac{v^{(i)}_{,\theta z}}{r}+2(1-\upsilon_i)w^{(i)}_{,zz}+(1-2\upsilon_i)w^{(i)}_{,rr}+\frac{1-2\upsilon_i}{r}w^{(i)}_{,r}+\frac{1-2\upsilon_i}{r^2}w^{(i)}_{,\theta\theta}=0 \tag{1c}$$

where $u^{(i)}$, $v^{(i)}$ and $w^{(i)}$ are displacement components of each body i ($i=1$ or 2) in the r, θ and z directions, respectively; υ_i is Poisson's ratio for material i; and the subscripts denote partial differentials with respect to the independent variables r, θ and z.

Since the problems under consideration here are for bodies of revolution, the solutions of Eqs. (1a)–(1c) are periodic in θ and may be expressed in terms of Fourier components in θ:

$$u^{(i)}=\sum_{n=0,1}U^{(i)}_n(r,z)\cos n\theta,\quad v^{(i)}=\sum_{n=1,2}V^{(i)}_n(r,z)\sin n\theta\quad\text{and}\quad w^{(i)}=\sum_{n=0,1}W^{(i)}_n(r,z)\cos n\theta \tag{2}$$

The geometry of any plane with fixed θ is as shown in Fig. 2. Substituting Eq. (2) into Eqs. (1a)–(1c), transforming (r, z) coordinates to (ρ, ϕ) coordinates as shown in Fig. 2 through

$$\rho=\sqrt{(r-R)^2+z^2},\quad \phi=\tan^{-1}\left(\frac{-z}{r-R}\right)+\beta,\quad r-R=\rho\cos(\phi-\beta),\ \text{and}\ z=-\rho\sin(\phi-\beta), \tag{3}$$

and substituting

$$U^{(i)}_n(\rho,\phi)=\sum_{m=0,1}^{\infty}\rho^{\lambda+m}\hat{U}^{(i)}_{nm}(\phi),\quad V^{(i)}_n(\rho,\phi)=\sum_{m=0,1}^{\infty}\rho^{\lambda+m}\hat{V}^{(i)}_{nm}(\phi),\quad W^{(i)}_n(\rho,\phi)=\sum_{m=0,1}^{\infty}\rho^{\lambda+m}\hat{W}^{(i)}_{nm}(\phi), \tag{4}$$

where λ can be a complex number, into the resulting equations, one obtains the following equations for the least power order of ρ:

$$[\lambda(\lambda-1)\cos^2\bar{\phi}+\lambda^2(1-2\upsilon_i)+\lambda\sin^2\bar{\phi}]\hat{U}^{(i)}_{n0}-(\lambda-1)\sin 2\bar{\phi}\hat{U}^{(i)}_{n0,\phi}+(\sin^2\bar{\phi}+1-2\upsilon_i)\hat{U}^{(i)}_{n0,\phi\phi}+\sin\bar{\phi}\cos\bar{\phi}\hat{W}^{(i)}_{n0,\phi\phi}+(1-\lambda)\cos 2\bar{\phi}\hat{W}^{(i)}_{n0,\phi}+\lambda(2-\lambda)\sin\bar{\phi}\cos\bar{\phi}\hat{W}^{(i)}_{n0}=0 \tag{5a}$$

$$\hat{V}^{(i)}_{n0,\phi\phi}+\lambda^2\hat{V}^{(i)}_{n0}=0, \tag{5b}$$

$$\lambda(2-\lambda)\sin\bar{\phi}\cos\bar{\phi}\hat{U}^{(i)}_{n0}+(1-\lambda)\cos 2\bar{\phi}\hat{U}^{(i)}_{n0,\phi}+\sin\bar{\phi}\cos\bar{\phi}\hat{U}^{(i)}_{n0,\phi\phi}+[\lambda(\lambda-1)\sin^2\bar{\phi}+\lambda^2(1-2\upsilon_i)+\lambda\cos^2\bar{\phi}]\hat{W}^{(i)}_{n0}+(\lambda-1)\sin 2\bar{\phi}\hat{W}^{(i)}_{n0,\phi}+(\cos^2\bar{\phi}+1-2\upsilon_i)\hat{W}^{(i)}_{n0,\phi\phi}=0, \tag{5c}$$

where $\bar{\phi}=\phi-\beta$, and β is the angle from a horizontal line to the axis of $\phi=0$. Since stress singularities at $\rho\to 0$ are investigated, only the solutions corresponding to the least power order of ρ are needed. More details of the above derivation can be found in Huang and Leissa [29].

The solution of Eq. (5b) is simply

$$\hat{V}^{(i)}_{n0}=A^{(i)}_1\cos\lambda\phi+A^{(i)}_2\sin\lambda\phi, \tag{6}$$

where $A^{(i)}_1$ and $A^{(i)}_2$ are coefficients to be determined from boundary conditions.

Equations (5a) and (5b) are a set of coupled differential equations with variable coefficients. To find a closed form solution, one can perform the following transformation:

$$\hat{U}^{(i)}_{n0}(\phi)=\cos\bar{\phi}\bar{U}^{(i)}_{n0}(\phi)-\sin\bar{\phi}\bar{W}^{(i)}_{n0}(\phi), \tag{7a}$$

$$\hat{W}^{(i)}_{n0}(\phi)=-\sin\bar{\phi}\bar{U}^{(i)}_{n0}(\phi)-\cos\bar{\phi}\bar{W}^{(i)}_{n0}(\phi). \tag{7b}$$

Applying Eqs. (7a) and (7b) to Eqs. (5a) and (5b) and arranging the equations as Huang and Leissa [29] did, one obtains the solution,

$$\bar{U}^{(i)}_{n0}(\phi)=B^{(i)}_1\sin(\lambda+1)\phi-B^{(i)}_2\cos(\lambda+1)\phi+\gamma_iB^{(i)}_3\sin(\lambda-1)\phi-\gamma_iB^{(i)}_4\cos(\lambda-1)\phi, \tag{8a}$$

$$\bar{W}^{(i)}_{n0}(\phi)=B^{(i)}_1\cos(\lambda+1)\phi+B^{(i)}_2\sin(\lambda+1)\phi+B^{(i)}_3\cos(\lambda-1)\phi+B^{(i)}_4\sin(\lambda-1)\phi, \tag{8b}$$

where $\gamma_i=(-3+\lambda+4\upsilon_i)/(3+\lambda-4\upsilon_i)$, and $B^{(i)}_j$ (j=1, 2, 3, 4) are coefficients to be determined from boundary conditions.

As a brief summary, the solutions of Eqs. (1) are

$$u^{(i)}(\rho,\phi,\theta)=\sum_n\rho^{\lambda}(\cos(\phi-\beta)\bar{U}^{(i)}_{n0}(\phi)-\sin(\phi-\beta)\bar{W}^{(i)}_{n0}(\phi))\cos n\theta+O(\rho^{\lambda+1}), \tag{9a}$$

$$v^{(i)}(\rho,\phi,\theta)=\sum_n\rho^{\lambda}(A^{(i)}_1\cos\lambda\phi+A^{(i)}_2\sin\lambda\phi)\sin n\theta+O(\rho^{\lambda+1}), \tag{9b}$$

$$w^{(i)}(\rho,\phi,\theta)=\sum_n\rho^{\lambda}(-\sin(\phi-\beta)\bar{U}^{(i)}_{n0}(\phi)-\cos(\phi-\beta)\bar{W}^{(i)}_{n0}(\phi))\cos n\theta+O(\rho^{\lambda+1}), \tag{9c}$$

where $O(\rho^{\lambda+1})$ includes all the terms of order in ρ higher than λ. Notably, the real part of λ has to exceed unity to meet the requirement of finite deformations. Using Eqs. (9), the strain–displacement relations, and stress–strain relations, one obtains, after some manipulation, the stress components expressed as

$$\tau^{(i)}_{r\theta}=\sum_n G_i\lambda\rho^{\lambda-1}[\cos((\lambda-1)\phi+\beta)A^{(i)}_1+\sin((\lambda-1)\phi+\beta)A^{(i)}_2]\sin n\theta+O(\rho^{\lambda}), \tag{10a}$$

$$\tau^{(i)}_{z\theta}=\sum_n G_i\lambda\rho^{\lambda-1}[\sin((\lambda-1)\phi+\beta)A^{(i)}_1-\cos((\lambda-1)\phi+\beta)A^{(i)}_2]\sin n\theta+O(\rho^{\lambda}), \tag{10b}$$

$$\tau^{(i)}_{rz}=\sum_n-2\lambda G_i\rho^{\lambda-1}\{\cos((\lambda-1)\phi+2\beta)B^{(i)}_1+\sin((\lambda-1)\phi+2\beta)B^{(i)}_2+\frac{\lambda-1}{3+\lambda-4\upsilon_i}[\cos((\lambda-3)\phi+2\beta)B^{(i)}_3+\sin((\lambda-3)\phi+2\beta)B^{(i)}_4]\}\cos n\theta+O(\rho^{\lambda}), \tag{10c}$$

$$\sigma_{rr}^{(i)} = \sum_n 2\lambda G_i \rho^{\lambda-1}\{\sin((\lambda-1)\phi+2\beta)B_1^{(i)} - \cos((\lambda-1)\phi+2\beta)B_2^{(i)} + \frac{1}{3+\lambda-4\upsilon_i}[(-2\sin(\lambda-1)\phi + (\lambda-1)\sin((\lambda-3)\phi+2\beta))B_3^{(i)} + (2\cos(\lambda-1)\phi - (\lambda-1)\cos((\lambda-3)\phi+2\beta))B_4^{(i)}]\}\cos n\theta + O(\rho^{\lambda}), \quad (10d)$$

$$\sigma_{zz}^{(i)} = \sum_n 2\lambda G_i \rho^{\lambda-1}\{-\sin((\lambda-1)\phi+2\beta)B_1^{(i)} + \cos((\lambda-1)\phi+2\beta)B_2^{(i)} - \frac{1}{3+\lambda-4\upsilon_i}[(2\sin(\lambda-1)\phi + (\lambda-1)\sin((\lambda-3)\phi+2\beta))B_3^{(i)} - (2\cos(\lambda-1)\phi + (\lambda-1)\cos((\lambda-3)\phi+2\beta))B_4^{(i)}]\}\cos n\theta + O(\rho^{\lambda}), \quad (10e)$$

$$\sigma_{\theta\theta}^{(i)} = \sum_n \frac{8\lambda\upsilon_i G_i}{3+\lambda-4\upsilon_i}\rho^{\lambda-1}[-\sin((\lambda-1)\phi)B_3^{(i)} + \cos((\lambda-1)\phi)B_4^{(i)}]\cos n\theta + O(\rho^{\lambda}), \quad (10f)$$

where G_i is the shear modulus for material i. The real part of λ is related to the singularity order of stresses, and its imaginary part describes the oscillatory behavior of the stresses. Obviously, when the real part of λ is less than one, stress singularities exist at $\rho = 0$.

3. Characteristic equations and corner functions

At corner A, considering free surfaces at $\phi = 0$ and $\phi = \alpha$ (see Fig. 2), the traction free conditions yield

$$\begin{aligned}&\sigma_{rr}^{(1)}\sin(-\beta) + \tau_{rz}^{(1)}\cos(-\beta_1) = 0,\\ &\tau_{zr}^{(1)}\sin(-\beta) + \sigma_{zz}^{(1)}\cos(-\beta) = 0,\\ &\tau_{\theta r}^{(1)}\sin(-\beta) + \tau_{\theta z}^{(1)}\cos(-\beta) = 0;\end{aligned} \quad (11a)$$

and

$$\begin{aligned}&\sigma_{rr}^{(2)}\sin(\alpha-\beta) + \tau_{rz}^{(2)}\cos(\alpha-\beta) = 0,\\ &\tau_{zr}^{(2)}\sin(\alpha-\beta) + \sigma_{zz}^{(2)}\cos(\alpha-\beta) = 0,\\ &\tau_{\theta r}^{(2)}\sin(\alpha-\beta) + \tau_{\theta z}^{(2)}\cos(\alpha-\beta) = 0.\end{aligned} \quad (11b)$$

The continuity conditions of displacements and tractions along the interface must also be satisfied. Hence, at $\phi = \alpha_1$

$$\begin{aligned}&u^{(1)} = u^{(2)}, \quad v^{(1)} = v^{(2)}, \quad w^{(1)} = w^{(2)}\\ &\sigma_{rr}^{(1)}\sin(\alpha_1-\beta) + \tau_{rz}^{(1)}\cos(\alpha_1-\beta)\\ &\quad = \sigma_{rr}^{(2)}\sin(\alpha_1-\beta) + \tau_{rz}^{(2)}\cos(\alpha_1-\beta)\\ &\qquad \times \tau_{zr}^{(1)}\sin(\alpha_1-\beta) + \sigma_{zz}^{(1)}\cos(\alpha-\beta)\\ &\quad = \tau_{zr}^{(2)}\sin(\alpha_1-\beta) + \sigma_{zz}^{(2)}\cos(\alpha_1-\beta)\\ &\qquad \times \tau_{\theta r}^{(1)}\sin(\alpha_1-\beta) + \tau_{\theta z}^{(1)}\cos(\alpha_1-\beta)\\ &\quad = \tau_{\theta r}^{(2)}\sin(\alpha_1-\beta) + \tau_{\theta z}^{(2)}\cos(\alpha_1-\beta),\end{aligned} \quad (11c)$$

Substituting Eqs. (9) and (10) into Eqs. (11) and considering the least power order of ρ in the resulting equations yields, after some intensive manipulation,

$$\cos\beta B_1^{(1)} + \sin\beta B_2^{(1)} + \frac{\lambda-1}{3+\lambda-4\upsilon_1}\cos\beta B_3^{(1)} + \frac{\lambda+1}{3+\lambda-4\upsilon_1}\sin\beta B_4^{(1)} = 0 \quad (12a)$$

$$-\sin\beta B_1^{(1)} + \cos\beta B_2^{(1)} - \frac{\lambda-1}{3+\lambda-4\upsilon_1}\sin\beta B_3^{(1)} + \frac{\lambda+1}{3+\lambda-4\upsilon_1}\cos\beta B_4^{(1)} = 0 \quad (12b)$$

$$A_2^{(1)} = 0 \quad (12c)$$

$$\begin{aligned}&\cos(\lambda\alpha+\beta)B_1^{(2)} + \sin(\lambda\alpha+\beta)B_2^{(2)}\\ &\quad + \frac{1}{3+\lambda-4\upsilon_2}\{[2\sin(\alpha-\beta)\sin((\lambda-1)\alpha) + (\lambda-1)\\ &\quad \times\cos((\lambda-2)\alpha+\beta)]B_3^{(2)} + [-2\sin(\alpha-\beta)\cos((\lambda-1)\alpha)\\ &\quad + (\lambda-1)\sin((\lambda-2)\alpha+\beta)]B_4^{(2)}\} = 0\end{aligned} \quad (12d)$$

$$\begin{aligned}&-\sin(\lambda\alpha+\beta)B_1^{(2)} + \cos(\lambda\alpha+\beta)B_2^{(2)}\\ &\quad + \frac{1}{3+\lambda-4\upsilon_2}\{-[2\cos(\alpha-\beta)\sin((\lambda-1)\alpha) + (\lambda-1)\\ &\quad \times\sin((\lambda-2)\alpha+\beta)]B_3^{(2)} + [2\cos(\alpha-\beta)\cos((\lambda-1)\alpha)\\ &\quad + (\lambda-1)\cos((\lambda-2)\alpha+\beta)]B_4^{(2)}\} = 0\end{aligned} \quad (12e)$$

$$\sin(\lambda\alpha)A_1^{(2)} - \cos(\lambda\alpha)A_2^{(2)} = 0 \quad (12f)$$

$$\begin{aligned}&\sin((\lambda+1)\alpha_1)B_1^{(1)} - \cos((\lambda+1)\alpha_1)B_2^{(1)}\\ &\quad + \gamma_1\sin((\lambda-1)\alpha_1)B_3^{(1)} - \gamma_1\cos((\lambda-1)\alpha_1)B_4^{(1)}\\ &\quad = \sin((\lambda+1)\alpha_1)B_1^{(2)} - \cos((\lambda+1)\alpha_1)B_2^{(2)}\\ &\quad + \gamma_2\sin((\lambda-1)\alpha_1)B_3^{(2)} - \gamma_2\cos((\lambda-1)\alpha_1)B_4^{(2)}\end{aligned} \quad (12g)$$

$$\begin{aligned}&\cos(\lambda\alpha_1)A_1^{(1)} + \sin(\lambda\alpha_1)A_2^{(1)}\\ &\quad = \cos(\lambda\alpha_1)A_1^{(2)} + \sin(\lambda\alpha_1)A_2^{(2)}\end{aligned} \quad (12h)$$

$$\begin{aligned}&\cos((\lambda+1)\alpha_1)B_1^{(1)} + \sin((\lambda+1)\alpha_1)B_2^{(1)}\\ &\quad + \cos((\lambda-1)\alpha_1)B_3^{(1)} + \sin((\lambda-1)\alpha_1)B_4^{(1)}\\ &\quad = \cos((\lambda+1)\alpha_1)B_1^{(2)} + \sin((\lambda+1)\alpha_1)B_2^{(2)}\\ &\quad + \cos((\lambda-1)\alpha_1)B_3^{(2)} + \sin((\lambda-1)\alpha_1)B_4^{(2)}\end{aligned} \quad (12i)$$

$$\begin{aligned}&\frac{E_1}{1+\upsilon_1}\Big\{-\cos(\lambda\alpha_1+\beta)B_1^{(1)} - \sin(\lambda\alpha_1+\beta)B_2^{(1)}\\ &\quad - \frac{1}{3+\lambda-4\upsilon_1}[(2\sin(\alpha_1-\beta)\sin((\lambda-1)\alpha_1) + (\lambda-1)\\ &\quad \times\cos((\lambda-2)\alpha_1+\beta))B_3^{(1)} + (2\sin(\alpha_1-\beta)\cos((\lambda-1)\alpha_1)\\ &\quad -(\lambda-1)\sin((\lambda-2)\alpha_1+\beta))B_4^{(1)}]\Big\}\\ &= \frac{E_2}{1+\upsilon_2}\Big\{-\cos(\lambda\alpha_1+\beta)B_1^{(2)} - \sin(\lambda\alpha_1+\beta)B_2^{(2)}\\ &\quad - \frac{1}{3+\lambda-4\upsilon_2}[(2\sin(\alpha_1-\beta)\sin((\lambda-1)\alpha_1)\\ &\quad +(\lambda-1)\cos((\lambda-2)\alpha_1+\beta))B_3^{(2)} - (2\sin(\alpha_1-\beta)\\ &\quad \times\cos((\lambda-1)\alpha_1) - (\lambda-1)\sin((\lambda-2)\alpha_1+\beta))B_4^{(2)}]\Big\}\end{aligned} \quad (12j)$$

$$\frac{E_1}{1+\upsilon_1}\Big\{-\sin(\lambda\alpha_1+\beta)B_1^{(1)}+\cos(\lambda\alpha_1+\beta)B_2^{(1)} + \frac{1}{3+\lambda-4\upsilon_1}[-(2\cos(\alpha_1-\beta)\sin((\lambda-1)\alpha_1) + (\lambda-1)\sin((\lambda-2)\alpha_1+\beta))B_3^{(1)} + (2\cos(\alpha_1-\beta) \times\cos((\lambda-1)\alpha_1)+(\lambda-1)\cos((\lambda-2)\alpha_1+\beta))B_4^{(1)}]\Big\} = \frac{E_2}{1+\upsilon_2}\Big\{-\sin(\lambda\alpha_1+\beta)B_1^{(2)}+\cos(\lambda\alpha_1+\beta)B_2^{(2)} + \frac{1}{3+\lambda-4\upsilon_2}[-(2\cos(\alpha_1-\beta)\sin((\lambda-1)\alpha_1)+(\lambda-1) \times\sin((\lambda-2)\alpha_1+\beta))B_3^{(2)} + (2\cos(\alpha_1-\beta)\cos((\lambda-1)\alpha_1) +(\lambda-1)\cos((\lambda-2)\alpha_1+\beta))B_4^{(2)}]\Big\} \tag{12k}$$

$$G_1\{\sin(\lambda\alpha_1)A_1^{(1)}-\cos(\lambda\alpha_1)A_2^{(1)}\} = G_2\{\sin(\lambda\alpha_1)A_1^{(2)}-\cos(\lambda\alpha_1)A_2^{(2)}\} \tag{12l}$$

To have nontrivial solutions for $A_k^{(i)}$, Eqs. (12f), (12h), and (12l) yield a third order determinant equal to zero, and thus λ has to satisfy

$$-(1+G_r)\sin\lambda\alpha+(1-G_r)\sin(\lambda(\alpha-2\alpha_1))=0, \tag{13a}$$

where $G_r=G_2/G_1$. Similarly, to obtain nontrivial solutions for $B_j^{(i)}$, Eqs. (12) involving $B_j^{(i)}$ yield an eight order determinant equal to zero, and λ has to satisfy

$$\begin{aligned}&\delta_0+\delta_1\cos 2\alpha+\delta_2\cos 2\lambda\alpha+\delta_3\cos 2(\alpha-2\alpha_1)\\&\quad+\delta_4\cos 2\lambda(\alpha-2\alpha_1)+\delta_5\cos 2(\lambda\alpha-(1+\lambda)\alpha_1)\\&\quad+\delta_6\cos 2(\alpha-\alpha_1)+\delta_7\cos 2\lambda(\alpha-\alpha_1)+\delta_8\cos 2\alpha_1\\&\quad+\delta_9\cos 2\lambda\alpha_1+\delta_{10}\cos 2(\alpha+(\lambda-1)\alpha_1)\\&\quad+\delta_5\cos 2(\lambda\alpha-(\lambda-1)\alpha_1)\\&\quad+\delta_{10}\cos 2(\alpha-(1+\lambda)\alpha_1)=0,\end{aligned} \tag{13b}$$

where

$$\begin{aligned}\delta_0&=-2(-1+\lambda^2)[-5+\lambda^2+G_r^2(-5+\lambda^2+12\upsilon_1-8\upsilon_1^2)\\&\quad+12\upsilon_2-8\upsilon_2^2-2G_r(-1+\lambda^2+2\upsilon_1+2\upsilon_2-4\upsilon_1\upsilon_2)]\\
\delta_1&=-\lambda^2[\lambda^2+G_r^2\lambda^2-2G_r(\lambda^2-8(-1+\upsilon_1)(-1+\upsilon_2))],\\
\delta_2&=-[-1+G_r(-3+4\upsilon_1)](3+G_r-4\upsilon_2),\\
\delta_3&=-\lambda^4(-1+G_r)^2,\\
\delta_4&=-(-1+G_r)[3+G_r(-3+4\upsilon_1)-4\upsilon_2],\\
\delta_5&=\lambda^2(-1+G_r)(3+G_r-4\upsilon_2),\\
\delta_6&=2\lambda^2[-1+\lambda^2+G_r^2(-5+\lambda^2+12\upsilon_1-8\upsilon_1^2)\\&\quad-2G_r(-3+\lambda^2+2\upsilon_1+4\upsilon_2-4\upsilon_1\upsilon_2)],\\
\delta_7&=-2[G_r^2(-5+\lambda^2+12\upsilon_1-8\upsilon_1^2)\\&\quad-2G_r(1+\lambda^2-2\upsilon_1)(-1+2\upsilon_2)+(-1+\lambda^2)(-3+4\upsilon_2)],\\
\delta_8&=2\lambda^2[-5+\lambda^2+G_r^2(-1+\lambda^2)+12\upsilon_2-8\upsilon_2^2\\&\quad-2G_r(-3+\lambda^2+4\upsilon_1+2\upsilon_2-4\upsilon_1\upsilon_2)],\\
\delta_9&=-2[-5+\lambda^2+G_r^2(-1+\lambda^2)(-3+4\upsilon_1)\\&\quad-2G_r(-1+2\upsilon_1)(1+\lambda^2-2\upsilon_2)+12\upsilon_2-8\upsilon_2^2],\\
\delta_{10}&=\lambda^2(-1+G_r)[-1+G_r(-3+4\upsilon_1)].\end{aligned}$$

The coefficients δ_i are independent of the boundary angles α_1 and α.

Eq. (13a) is the characteristic equation of λ in the solution for $v^{(i)}$, and determines the order of stress singularity for $\tau_{r\theta}$ and $\tau_{\theta z}$. Eq. (13b) is for the solution of $u^{(i)}$ and $w^{(i)}$, and determines stress singularities of the other stress components.

Having the characteristic equations, the eigenvalues λ can be determined from them. Substituting these eigenvalues into Eqs. (12), one can find the relations among coefficients $A_k^{(i)}$ and $B_j^{(i)}$, then obtains the corresponding asymptotic solutions (corner functions) by substituting the relations back into Eqs. (9). It is easy to find the asymptotic solutions for $v^{(i)}$. Eq. (12c), (12f), (12h), and (12l) result in

$$\begin{aligned}&A_2^{(1)}=0,\\&A_2^{(2)}=A_1^{(2)}\tan(\lambda\alpha_1),\quad A_1^{(1)}=A_1^{(2)}(1+\tan^2(\lambda\alpha_1)).\end{aligned} \tag{14}$$

4. Discussion of the solutions

The explicit general expressions of the corner functions for $u^{(i)}$ and $w^{(i)}$ are very complicated and lengthy, and will not be presented here. However, it is still desirable to have the expressions for some special combinations of α_1 and α (see Fig. 2) that are commonly found in practical problems. For $\beta=0$ and $(\alpha_1,\ \alpha)=(\pi/2,3\pi/2),(\pi,3\pi/2)$, or $(\pi,2\pi)$ the relations among $B_j^{(i)}$ are expressed as

$$\begin{aligned}&B_1^{(1)}=\frac{\chi_1}{\Delta_1}B_4^{(2)},\quad B_2^{(1)}=\frac{\chi_2}{\Delta_1}B_4^{(2)},\quad B_3^{(1)}=\frac{\chi_3}{\Delta_1}B_4^{(2)},\\&B_4^{(1)}=\frac{\chi_4}{\Delta_1}B_4^{(2)},\quad B_1^{(2)}=\frac{\chi_5}{\Delta_1}B_4^{(2)},\quad B_2^{(2)}=\frac{\chi_6}{\Delta_1}B_4^{(2)},\ \text{and}\\&B_3^{(2)}=\frac{\chi_7}{\Delta_1}B_4^{(2)},\end{aligned}$$

where Δ_1 and χ_i $(i=1,2,\ldots 7)$ are listed in Table 1. These asymptotic solutions are shown here in the literature for the first time.

Carefully investigating the characteristic equations given in Eqs. (13), one will find they are equivalent to those published for plane elasticity and torsional problems. Through the use of trigonometric identities, Eq. (13a) is found to be equivalent to that given by Rao [30] for the St. Venant torsion of a bimaterial bar, and Eq. (13b) is equivalent to that given by Bogy [31] and Dempsey and Sinclair [32] for the plain strain problem of a bimaterial wedge with free boundary conditions along two radial edges.

Some numerical results for λ from Eqs. (13a) and (13b) were shown in Rao [30], Bogy [31], Hein and Erdogan [33], and Gdoutos and Theocaris [34]. Rao [30] plotted the results of λ obtained from Eq. (13a) on a $\lambda\alpha_1-\lambda\alpha_2$ plane with $G_r=1/2,\ 1,\ 3/2,\ 2,$ and 3, and also plotted the variation of λ from Eq. (13b) with α_1 for the case of $\alpha=2\alpha_1$. The contour lines of λ from Eq. (13b) were often plotted on a $\bar\alpha-\bar\beta$ plane, where $\bar\alpha=\frac{G_1m_2-G_2m_1}{G_1m_2+G_2m_1}$, $\bar\beta=\frac{G_1(m_2-2)-G_2(m_1-2)}{G_1m_2+G_2m_1}$ and $m_i=4(1-\upsilon_i)$ and $m_i=4/(1+\upsilon_i)$ for plane strain

Table 1
Expressions for and χ_i $(i = 1, 2, \ldots 7)$

α_1	α	Δ_1 and χ_i $(i = 1, 2, \ldots 7)$
		$\Delta_1 = 1 + G_r(3 - 4\upsilon_1) + 4(\upsilon_1 - \upsilon_2) + 8\lambda(-1 + \upsilon_2)(\lambda - 2(-1 + \upsilon_1)) + [1 + 4\lambda^2 - 8\lambda(-1 + \upsilon_1) - 4(2\upsilon_1 - \upsilon_2) + G_r(7 - 4\lambda^2 - 20\upsilon_1 + 16\upsilon_1^2)]\cos(\lambda\pi) + [-1 - 4\lambda^2 + 8\lambda(-1 + \upsilon_1) + 4\upsilon_1 - G_r(7 - 4\lambda^2 - 20\upsilon_1 + 16\upsilon_1^2)] \times \cos(2\lambda\pi) + [-1 + G_r(-3 + 4\upsilon_1)]\cos(3\lambda\pi)$
		$\chi_1 = 2(\lambda - 1)\tan(\lambda\pi/2)/(3 + \lambda - 4\upsilon_2)\{-(1 + \lambda)(5 - 12\upsilon_2 + 8\upsilon_2^2) + G_r[-3 + 2(\upsilon_1 + \upsilon_2) + \lambda(-3 + 4\upsilon_2)] + 4G_r(-1 + \upsilon_2)(2 + \lambda - 2\upsilon_1)\cos(\lambda\pi) + [(1 + \lambda)(-3 + 4\upsilon_2) - G_r(5 + \lambda - 6(\upsilon_1 + \upsilon_2) + 8\upsilon_1\upsilon_2)]\cos(2\lambda\pi)\}$
		$\chi_2 = 2(1 + \lambda)/(3 + \lambda - 4\upsilon_2)\{2G_r(\upsilon_2 - \upsilon_1) + \lambda[5 + G_r(3 - 4\upsilon_2) + 4\upsilon_2(2\upsilon_2 - 3)] + 4G_r(-1 + \upsilon_2)(1 + \lambda - 2\upsilon_1) \times \cos(\lambda\pi) + [\lambda(3 - 4\upsilon_2) + G_r(4 + \lambda - 6(\upsilon_1 + \upsilon_2) + 8\upsilon_1\upsilon_2)]\cos(2\lambda\pi)\}$
$\pi/2$	$3\pi/2$	
		$\chi_3 = -\chi_1(3 + \lambda - 4\upsilon_1)/(\lambda - 1)$
		$\chi_4 = -\chi_2(3 + \lambda - 4\upsilon_1)/(1 + \lambda)$
		$\chi_5 = \tan(\lambda\pi/2)/(3 + \lambda - 4\upsilon_2)\{-1 + G_r(1 + \lambda)(-3 + 4\upsilon_1) + \lambda[7 - 4(\upsilon_1 + \upsilon_2)] + 8\lambda^2(-1 + \upsilon_2)(\lambda - (-1 + 2\upsilon_2)) + [-3 - 4\lambda^3 + 4\upsilon_1 + G_r(1 + \lambda)(-13 + 4\lambda^2 + 28\upsilon_1 - 16\upsilon_1^2) + 4\lambda^2(1 + 2\upsilon_1 - 4\upsilon_2) + \lambda(-7 + 8\upsilon_1) \times (-3 + 4\upsilon_2)]\cos(\lambda\pi) + [-3 - 4\lambda^3 + G_r(1 + \lambda)(-13 + 4\lambda^2 + 28\upsilon_1 - 16\upsilon_1^2) + 4\lambda^2(1 + 2\upsilon_1 - 4\upsilon_2) + 4\upsilon_2 + \lambda(21 - 20\upsilon_1 - 32\upsilon_2 + 32\upsilon_1\upsilon_2)]\cos(2\lambda\pi) - [(-3 + 4\upsilon_1)(-3 + 4\upsilon_2 - G_r(1 + \lambda)) + \lambda]\cos(3\lambda\pi)\}$
		$\chi_6 = 1/(3 + \lambda - 4\upsilon_2)\{9 - 16\upsilon_1 - G_r(1 + \lambda)(-3 + 4\upsilon_1) - 8\upsilon_2(1 - 2\upsilon_1) + +8\lambda^2(-1 + \upsilon_2)(\lambda - (-1 + 2\upsilon_2)) + \lambda(17 - 20\upsilon_2 + 4\upsilon_1(-3 + 4\upsilon_2)) + [-15 + 4\lambda^3 + 28\upsilon_1 - G_r(1 + \lambda)(-7 + 4\lambda^2 + 20\upsilon_1 - 16\upsilon_1^2) - 4\lambda^2(1 + 2\upsilon_1 - 4\upsilon_2) + 16\upsilon_2(1 - 2\upsilon_1) + \lambda(-23 + 16\upsilon_1 + 36\upsilon_2 - 32\upsilon_1\upsilon_2)]\cos(\lambda\pi) + [-4\lambda^3 + G_r(1 + \lambda)(-7 + 4\lambda^2 + 20\upsilon_1 - 16\upsilon_1^2) + 4\lambda^2(1 + 2\upsilon_1 - 4\upsilon_2) + (-5 + 8\upsilon_1)(-3 + 4\upsilon_2) + \lambda(23 - 20\upsilon_1 - 32\upsilon_2 + 32\upsilon_1\upsilon_2)] \times \cos(2\lambda\pi) + [-\lambda + (-3 + 4\upsilon_1)(G_r(1 + \lambda) - (-3 + 4\upsilon_2))\cos(3\lambda\pi)\}$
		$\chi_7 = \tan(\lambda\pi/2)\{(G_r + 3 - 4\upsilon_2)(3 - 4\upsilon_1) - 8\lambda(-1 + \upsilon_2)(\lambda - 2(-1 + \upsilon_1)) + [3 + 4\lambda^2 - 4\upsilon_2 - 8\lambda(-1 + \upsilon_1) + G_r(13 - 4\lambda^2 - 28\upsilon_1 + 16\upsilon_1^2)]\cos(\lambda\pi) + [(1 + 2\lambda)(3 + 2\lambda - 4\upsilon_1) + G_r(13 - 4\lambda^2 - 28\upsilon_1 + 16\upsilon_1^2)] \times \cos(2\lambda\pi) + [1 + G_r(3 - 4\upsilon_1)]\cos(3\lambda\pi)\}$
		$\Delta_1 = (-1 + G_r)(-3 + 4\upsilon_1) + [3 - 4\upsilon_2 + 2\lambda(-3 + 4\upsilon_1) - G_r(-1 + 2\lambda)(13 - 28\upsilon_1 + 16\upsilon_1^2)]\cos(\lambda\pi) - 2[1 - 2\upsilon_1 + G_r(5 - 12\upsilon_1 + 8\upsilon_1^2)]\cos(2\lambda\pi) + [-3 + 4\upsilon_2 + 2\lambda(3 - 4\upsilon_1) + G_r(-1 + 2\lambda)(-3 + 4\upsilon_1)]\cos(3\lambda\pi) + [-1 + G_r(-3 + 4\upsilon_1)]\cos(4\lambda\pi)$
		$\chi_1 = 4(\lambda - 1)\sin(\lambda\pi)/(3 + \lambda - 4\upsilon_2)\{2\lambda^2 - 5 + 12\upsilon_2 - 8\upsilon_2^2 - G_r(-1 + 2\upsilon_1)(1 - 2\upsilon_2 + 4\lambda(-1 + \upsilon_2) + 2\lambda^2) + [-3 + 4\upsilon_2 + G_r(-5 + 6\upsilon_2 + 2\upsilon_1(3 - 4\upsilon_2))]\cos(\lambda\pi)$

(*continued on next page*)

Table 1 (*Continued*)

α_1	α	Δ_1 and χ_i $(i = 1, 2, \ldots 7)$
		$\chi_2 = 4G_r(1+\lambda)/(3+\lambda-4\upsilon_2)\{-(\upsilon_2-\upsilon_1)+2(-1+\upsilon_1)(1-2\upsilon_2+4\lambda(-1+\upsilon_2)+2\lambda^2)\cos(\lambda\pi)+(2-3\upsilon_2+\upsilon_1(-3+4\upsilon_2))\cos(2\lambda\pi)\}$
		$\chi_3 = -\chi_1(3+\lambda-4\upsilon_1)/(\lambda-1)$
		$\chi_4 = -\chi_2(3+\lambda-4\upsilon_1)/(1+\lambda)$
π	$3\pi/2$	
		$\chi_5 = 2\sin(\lambda\pi)/(3+\lambda-4\upsilon_2)\{-1+G_r(1+\lambda-2\lambda^2)(5-12\upsilon_1+8\upsilon_1^2)-\lambda(-3+4\upsilon_1)(-3+4\upsilon_2)+2\lambda^2+[-3+4\upsilon_2-\lambda(-3+4\upsilon_1)+G_r(-1+\lambda)(13-28\upsilon_1+16\upsilon_1^2)]\cos(\lambda\pi)+[-3+4\upsilon_1+\lambda(-3+4\upsilon_2)+2\lambda^2(3-4\upsilon_1)+G_r(-3+4\upsilon_1)(-1-\lambda+2\lambda^2)]\cos(2\lambda\pi)-[(-3+4\upsilon_1)(-3+4\upsilon_2)-\lambda+G_r(-1+\lambda)(-3+4\upsilon_1)]\cos(3\lambda\pi)\}$
		$\chi_6 = 1/(3+\lambda-4\upsilon_2)\{3-4\upsilon_2-G_r(-1+\lambda)(-3+4\upsilon_1)+\lambda(-3+4\upsilon_1)+[3-4\upsilon_1-\lambda(-3+4\upsilon_2)+2\lambda^2(-3+4\upsilon_1)-G_r(-1-\lambda+2\lambda^2)(13-28\upsilon_1+16\upsilon_1^2)]\cos(\lambda\pi)+2[G_r(-1+\lambda)(5-12\upsilon_1+8\upsilon_1^2)-(-1+2\upsilon_1)\times(3+\lambda-4\upsilon_2)]\cos(2\lambda\pi)+[-3+4\upsilon_1+\lambda(-3+4\upsilon_2)+2\lambda^2(3-4\upsilon_1)+G_r(-3+4\upsilon_1)(-1-\lambda+2\lambda^2)]\times\cos(3\lambda\pi)-[(-3+4\upsilon_1)(-3+4\upsilon_2)-\lambda+G_r(-1+\lambda)(-3+4\upsilon_1)]\cos(4\lambda\pi)$
		$\chi_7 = 2\sin(\lambda\pi)\{(-3+4\upsilon_2)(-3+4\upsilon_1)-2\lambda+G_r(-1+2\lambda)(5-12\upsilon_1+8\upsilon_1^2)+[3-4\upsilon_1+G_r(13-28\upsilon_1+16\upsilon_1^2)]\cos(\lambda\pi)+[3-4\upsilon_2+2\lambda(-3+4\upsilon_1)-G_r(-1+2\lambda)(-3+4\upsilon_1)]\cos(2\lambda\pi)+[1+G_r(3-4\upsilon_1)]\times\cos(3\lambda\pi)\}$
		$\Delta_1 = 4\sin(2\lambda\pi)\{3-2(\upsilon_1+\upsilon_2)+G_r(8\upsilon_1^2-12\upsilon_1+5)+[1+G_r(3-4\upsilon_1)]\cos(2\lambda\pi)\}$
		$\chi_1 = -4(\lambda-1)/(3+\lambda-4\upsilon_2)\{5-12\upsilon_2+8\upsilon_2^2+G_r[3-2(\upsilon_1+\upsilon_2)]+[3-4\upsilon_2+G_r(5-6(\upsilon_1+\upsilon_2)+8\upsilon_1\upsilon_2)]\times\cos(2\lambda\pi)\}$
		$\chi_2 = -8G_r(1+\lambda)/(3+\lambda-4\upsilon_2)[2-3\upsilon_2+\upsilon_1(-3+4\upsilon_2)]\sin(2\lambda\pi)$
		$\chi_3 = -\chi_1(3+\lambda-4\upsilon_1)/(\lambda-1)$
π	2π	
		$\chi_4 = -\chi_2(3+\lambda-4\upsilon_1)/(1+\lambda)$
		$\chi_5 = 2/(3+\lambda-4\upsilon_2)\{-1+\lambda(-3+4\upsilon_1)(-3+4\upsilon_2)-G_r(-1+\lambda)(-3+4\upsilon_1)+2(-1+\lambda)[3-2(\upsilon_1+\upsilon_2)+G_r(5-12\upsilon_1+8\upsilon_1^2)]\cos(2\lambda\pi)-[(-3+4\upsilon_1)(-3+4\upsilon_2)-\lambda+G_r(-1+\lambda)(-3+4\upsilon_1)]\cos(4\lambda\pi)\}$

Table 1 (*Continued*)

α_1	α	Δ_1 and χ_i $(i = 1, 2, \ldots 7)$

$$\chi_6 = -4\sin(2\lambda\pi)/(3+\lambda-4\upsilon_2)\{(-1+\lambda)[3-2(\upsilon_1+\upsilon_2)+G_r(5-12\upsilon_1+8\upsilon_1^2)]-[(-3+4\upsilon_1)(-3+4\upsilon_2) - \lambda + G_r(-1+\lambda)(-3+4\upsilon_1)]\cos(2\lambda\pi)\}$$

$$\chi_7 = 2\{-(-3+4\upsilon_1)(3-4\upsilon_2+G_r)+2[3-2(\upsilon_1+\upsilon_2)+G_r(5-12\upsilon_1+8\upsilon_1^2)]\cos(2\lambda\pi)+[1+G_r(3-4\upsilon_1)] \times \cos(4\lambda\pi)\}$$

and plane stress problems, respectively. Bogy [31] considered $\alpha_1 = 50°, 75°, 90°, 120°, 160°, 180°$ with $\alpha = 2\alpha_1$; $\alpha_1 = 20°, 45°, 60°$ with $\alpha = \pi$; $\alpha_1 = 45°, 90°, 135°$ with $\alpha = 2\pi$; and $\alpha_1 = \pi$ with $\alpha = 3\pi/2$. Gdoutos and Theocaris [34] studied the cases of $\alpha_1 = \pi$ with $\alpha = 240°$, 300°and 330°. Hein and Erdogan [33] investigated the values of the real part of λ varying with Young's modulus ratio and having Poisson's ratios equal to 0.2 and considering $\alpha = \pi$ with $\alpha_1 = 5°, 30°, 45°, 60°, 75°, 90°$; and $\alpha_1 = 5°, 30°, 45°, 60°, 75°, 90°, 105°, 120°, 135°, 150°, 165°, 180°$ with $\alpha = 180° + \alpha_1$. However, no corner function was shown for these torsion or plane problems in these previous works.

The aforementioned published results showing the contour lines of λ on $\bar{\alpha} - \bar{\beta}$ planes for sparsely discrete α_1 and α are useful for studying the variation of λ with material properties, but do not clearly show the variation of λ with α_1 or α_2 (equal to $\alpha - \alpha_1$). Hence, the present work will emphasize studies for the minimum real part of λ varying with α_1 or α_2.

Fig. 3 shows the variations of λ with α_1 for $\alpha = 2\pi$ and $E_r(= E_2/E_1) = 0.01, 0.1, 0.5$, and 1. Since Eqs. (13a) and (13b) are independent and yield different asymptotic solutions, two sets of curves are shown in Fig. 3. One set, arising from Eq. (13a), can apply to the torsion problem. The other set, generated by Eq. (13b), can apply to plane strain problems. In a general three dimensional elasticity problem of a biomaterial body of revolution, the singularity orders of different stress components are determined by one of these two equations.

Similarly, Fig. 4 shows the variation of the minimum real part of λ with α_2 (equal to $\alpha - \alpha_1$) for $\alpha_1 = \pi$ and $E_r = 0.1, 0.5, 1, 2, 10$, while Fig. 5 shows the results for $\alpha_1 = \pi/2$. Finally, Fig. 6 displays the effects of Poisson's ratios on the minimum real part of λ, where curves 1 and 2 are obtained from Eq. (13a), and curves 3 and 4 are from Eq. (13b).

Notably, the data shown in Figs. 3–5 were obtained by setting Poisson's ratios equal to 0.3. The cusps in the curves in Figs. 3–6 are due to the transition between real and complex values of λ.

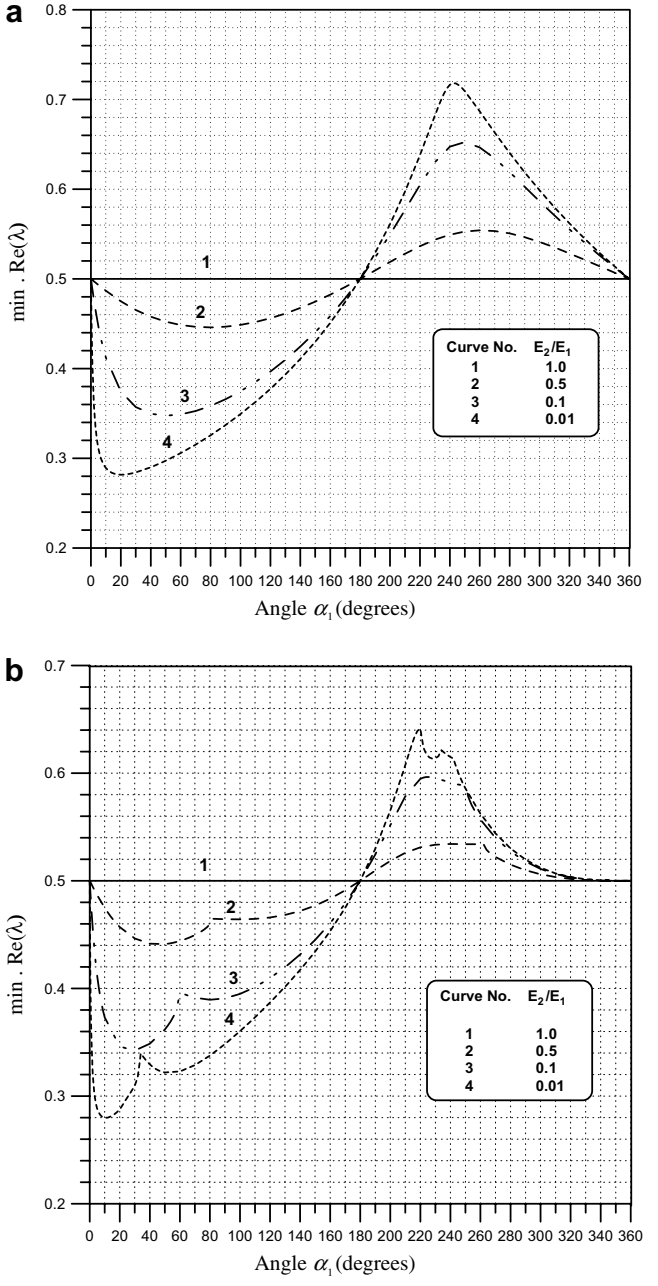

Fig. 3. Variation of minimum $Re(\lambda)$ with α_1 for $\alpha = 360°$: (a) obtained from Eqs. (13a); (b) obtained from Eq. (13b).

When $\alpha = 2\pi$, which is like an interface crack, the value of λ for $(G_r, \alpha_1, \alpha_2)$ equal to $(\kappa, \vartheta_1, \vartheta_2)$ is identical to that for $(G_r, \alpha_1, \alpha_2)$ equal to $(1/\kappa, \vartheta_2, \vartheta_1)$ if two materials have the same Poisson's ratio. Fig. 3 shows that the stress singularities for $\alpha_1 > \pi$ are less severe than those for $\alpha_1 < \pi$ if $E_r < 1$. When $E_r \leqslant 1$, smaller E_r results in stronger stress singularities when $\alpha_1 < \pi$, and the opposite trend is found for $\alpha_1 > \pi$. When $\alpha_1 = \pi$, although minimum Re(λ) is equal to 0.5 and independent on E_r, λ obtained from Eq. (13b) is complex for $E_r \neq 1$.

When $\alpha_1 = \pi$, which represents a truncated cone bonded to a cylinder of other material, Fig. 4a depicts how the strength of the stress singularities of $\tau_{r\theta}$ and $\tau_{\theta z}$ increases with increasing α_2, and the stress singularities become more severe for larger E_2/E_1. However, Fig. 4b shows that the strength of the stress singularities of τ_{rz}, σ_{rr}, σ_{zz}, and $\sigma_{\theta\theta}$ increases as α_2 increases from zero to a curtain angle depending on E_2/E_1, and when α_2 continues to increase, the strength of the stress singularities decreases somewhat, then increases further. Notably, the real part of λ is never smaller than 0.5.

When $\alpha_1 = \pi/2$, Fig. 5a shows no stress singularities exist for $\tau_{r\theta}$ and $\tau_{\theta z}$ when $\alpha_2 \leqslant 90°$, and the strength of

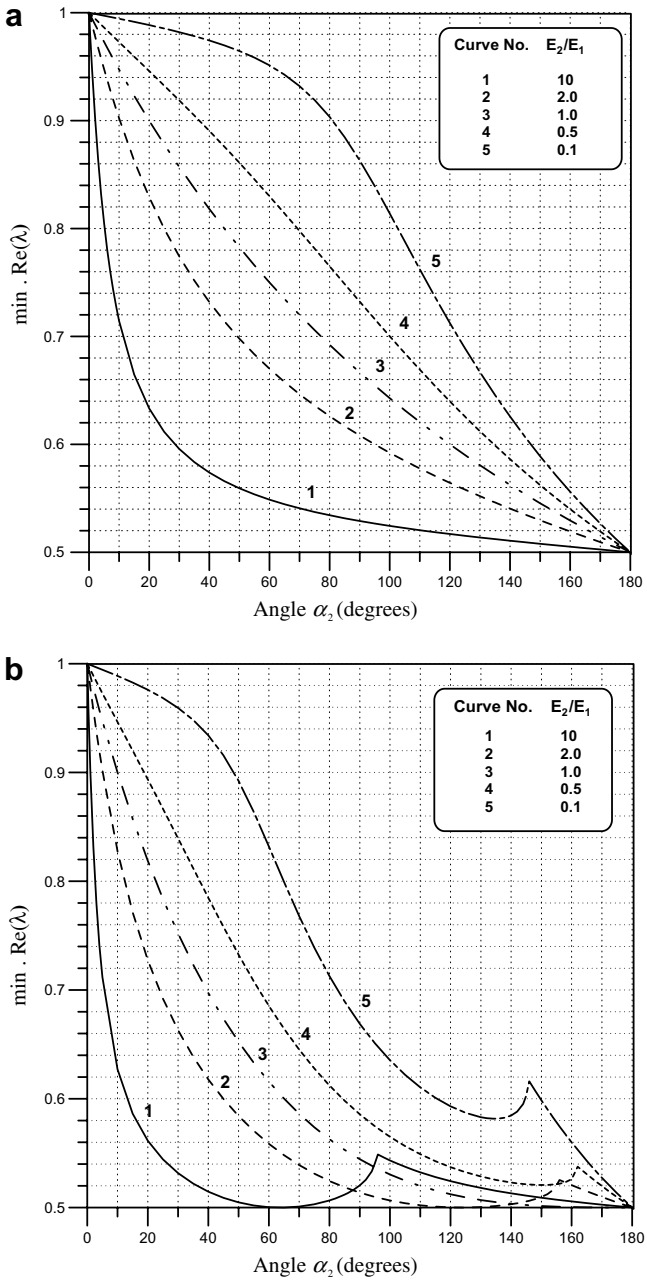

Fig. 4. Variation of minimum $Re(\lambda)$ with α_2 for $\alpha_1 = 180°$: (a) obtained from Eq. (13a); (b) obtained from Eq. (13b).

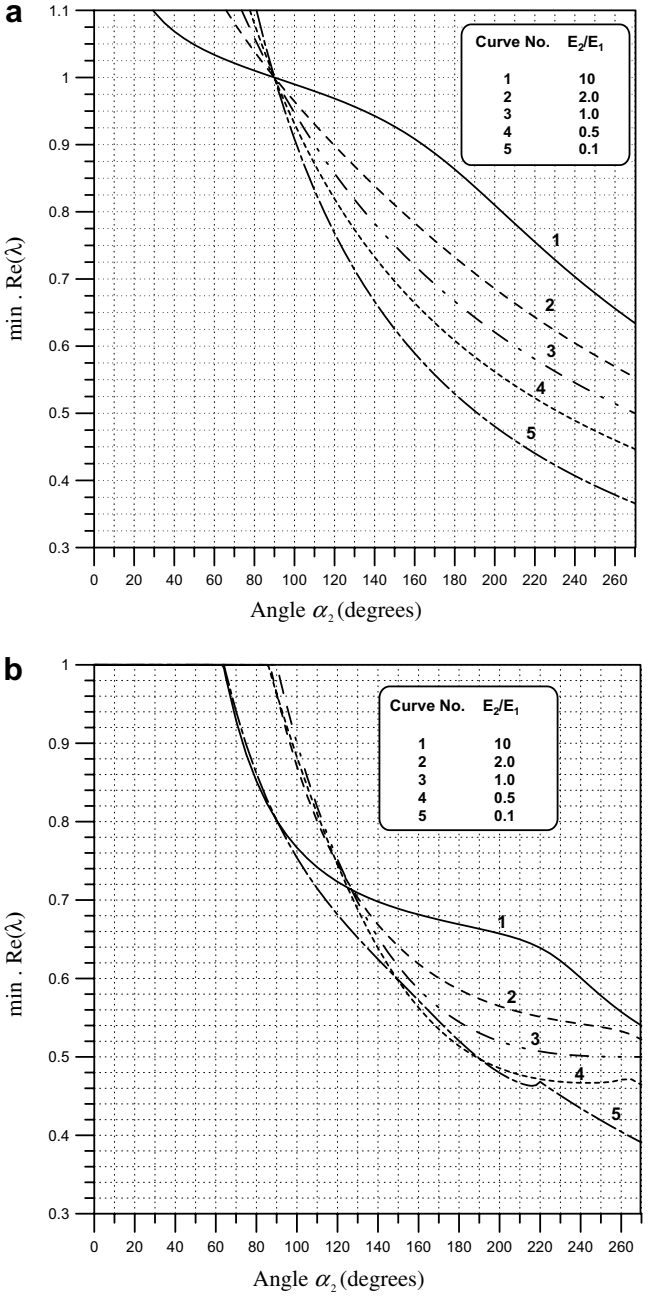

Fig. 5. Variation of minimum $Re(\lambda)$ with α_2 for $\alpha_1 = 90°$: (a) obtained from Eq. (13a); (b) obtained from Eq. (13b).

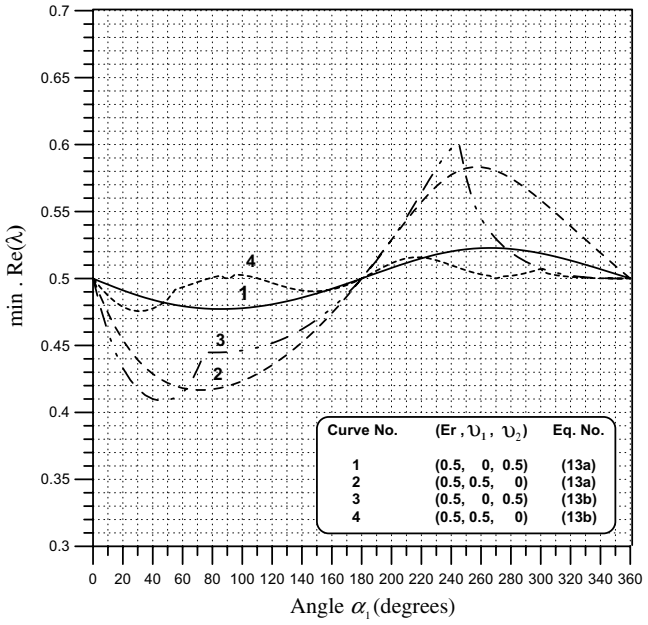

Fig. 6. The effect of Poisson's ratios on the minimum real part of λ.

the stress singularities increases with the increase of α_2 or the decrease of E_2/E_1. Fig. 5b displays there are no stress singularities for τ_{rz}, σ_{rr}, σ_{zz}, and $\sigma_{\theta\theta}$ when $\alpha_2 \leqslant 60^\circ$ and $0.1 \leqslant E_2/E_1 \leqslant 10$. Generally speaking, the stress singularities become more severe as α_2 increases.

Fig. 6 demonstrates the effects of Poisson's ratios on the stress singularities, depending on α_1, when $\alpha = 2\pi$ and $E_r(= E_2/E_1) = 0.5$. The Poisson ratios are set equal to extreme values 0 or 0.5. It can be observed that (υ_1, υ_2) changing from (0, 0.5) to (0.5, 0) may result in stronger stress singularities of $\tau_{r\theta}$ and $\tau_{\theta z}$ and weaker stress singularities for the other stress components when $\alpha_1 < \pi$, while the opposite trend is found for $\alpha_1 > \pi$. The changes in the strength of stress singularities are less than 20%.

5. Concluding remarks

This study has developed the asymptotic displacement and singular stress fields in the vicinity of the interface corner of a bimaterial body of revolution with free boundary conditions along the corner, based on three-dimensional elasticity. The characteristic equations for determining the stress singularity orders are explicitly given. The asymptotic analysis was accomplished by using the eigenfunction expansion approach to solve the equilibrium equations in terms of displacement functions.

The asymptotic displacement and stress fields presented are the first known to appear in the literature, while the characteristic equations are found equivalent to a combination of the characteristic equations for plane strain problems and St. Venant torsion problems. To fill the gap of the published numerical results from the characteristic equations, the variations of stress singularity orders with angles α and α_1 in Fig. 2 were plotted for various material properties. These results are very useful for numerical analyses of static and dynamic stress and deformation of a body having a V-notch at the interface of two bodies of revolution with different material properties.

Notably, one may start the derivation by changing Eq. (2) to

$$u^{(i)} = \sum_{n=1,2} U_n^{(i)}(r,z)\sin n\theta,$$

$$v^{(i)} = \sum_{n=0,1} V_n^{(i)}(r,z)\cos n\theta \text{ and } w^{(i)} = \sum_{n=1,2} W_n^{(i)}(r,z)\sin n\theta.$$

Nevertheless, no new results will be obtained because the results shown here are independent of n.

Although this paper only investigated the free boundary conditions along the revolution interface corner, the solution would be straightforward to consider other combinations of boundary conditions (e.g. fixed-free, fixed-fixed, or sliding). The characteristic equations for these types of boundary conditions are expected to be also the combinations of the characteristic equations of plane elasticity and St. Venant torsion problems.

References

[1] Williams ML. Stress singularities resulting from various boundary conditions in angular corners of plates in extension. J Appl Mech 1952;19:526–8.
[2] Williams ML. Surface stress singularities resulting from various boundary conditions in angular corners of plates under bending. Proceedings of the first US national congress of applied mechanics. New York: ASME; 1952. p. 325–9.
[3] Barsoum RS. On the use of isoparametric finite elements in linear fracture mechanics. Int J Numer Methods Eng 1976;10(1):25–37.
[4] Belytschko T, Krongauz Y, Fleming M, Organ D, Liu WK. Smoothing and accelerated computations in the element free Galerkin method. J Comput Appl Math 1996;74(1):111–26.
[5] Fleming M, Chu YA, Moran B, Belytschko T. Enriched element-free Galerkin methods for crack tip fields. Int J Numer Methods Eng 1997;40(8):1483–504.
[6] Huang CS. Stress singularities at angular corners in first-order shear deformation plate theory. Int J Mech Sci 2003;45(1):1–20.
[7] McGee OG, Leissa AW, Huang CS. Vibrations of cantilevered skewed plates with corner stress singularities. Int J Numer Methods Eng 1992;35(2):409–24.
[8] Huang CS, Leissa AW, Chang MJ. Vibrations of skewed cantilevered triangular, trapezoidal and parallelogram Mindlin plates with considering corner stress singularities. Int J Numer Methods Eng 2005;62(13):1789–806.
[9] Sih GC. A review of the three-dimensional stress problem for a cracked plate. Int J Fract Mech 1971;7(1):39–61.
[10] Panasyuk VV, Andrejkiv AE, Stadnik MM. Basic mechanical concepts and mathematical techniques in application to three-dimensional crack problems, a review. Eng Fract Mech 1980;3(4):925–37.
[11] Panasyuk VV, Andrejkiv AE, Stadnik MM. Three-dimensional static crack problems solution (a review). Eng Fract Mech 1981;14(1):245–60.
[12] Ting TCT. Explicit solution and invariance of the singularities at an interface crack in anisotropic composites. Int J Solids Struct 1986;22(9):965–83.
[13] Barsoum RS, Chen TK. Three dimensional surface singularity of an interface crack. Int J Fract 1991;50(3):221–37.

[14] Ghahremani F, Shih CF. Corner singularities of three-dimensional planar interface cracks. J Appl Mech 1992;59(1):61–8.
[15] Su XM, Sun CT. On singular stress at the crack tip of a thick plate under in-plane loading. Int J Fract 1996;82(3):237–52.
[16] Gregory RD. The general form of the three-dimensional elastic field inside an isotropic plate with free faces. J Elasticity 1992;28(1):1–28.
[17] Chaudhuri RA, Xie M. A novel eigenfunction expansion solution for three-dimensional crack problems. Compos Sci Technol 2000;60(12–13):2565–80.
[18] Zak AR. Stresses in the vicinity of boundary discontinuities in bodies of revolution. J Appl Mech 1964;31:150–2.
[19] Aksentian OK. Singularities of the stress–strain state of a plate in the neighborhood of an edge. J Appl Math Mech 1967;31:193–202.
[20] Bažant ZP. Three-dimensional harmonic functions near termination or intersection of gradient singularity lines: a general numerical method. Int J Eng Sci 1974;12:221–43.
[21] Bažant ZP, Estenssoro LF. General numerical method for three-dimensional singularities in cracked or notched elastic solids. In: Proceedings of the 4th international conference on fracture. Eaterloo, Ontario, vol. 3; 1977. p. 371–85.
[22] Keer LM, Parihar KS. Singularity at the vertex of pyramidal notches with three equal angles. Quarter J Appl Math 1977;35(2):401–5.
[23] Somaratna N, Ting TCT. Three-dimensional stress singularities in anisotropic materials and composites. Int J Eng Sci 1986;24(7):1115–34.
[24] Ghahremani F. A numerical variational method for extracting 3D singularities. Int J Solids Struct 1991;27(11):1371–86.
[25] Picu CR, Gupta V. Three-dimensional stress singularities at the tip of a grain triple junction line intersecting the free surface. J Mech Phys Solids 1997;45(9):1495–520.
[26] Schmitz H, Volk K, Wendland W. Three-dimensional singularities of elastic fields near vertices. Numer Methods Partial Differential Equations 1993;9(3):323–37.
[27] Glushkov E, Glushkova N, Lapina O. 3-D elastic stress singularity at polyhedral corner points. Int J Solids Struct 1999;36(8):1105–28.
[28] Koguchi H, Muramoto T. The order of stress singularity near the vertex in three-dimensional joints. Int J Solids Struct 2000;37(35):4737–62.
[29] Huang CS, Leissa AW. Three-dimensional sharp corner displacement functions for bodies of revolution. J Appl Mech, ASME 2007;74(1):41–6.
[30] Rao AK. Stress concentrations and singularities at interface corners. Zeitschrift fur Angewandte Mathematik und Mechanik 1971;51:395–406.
[31] Bogy DB. Two edge-bonded elastic wedges of different materials and wedge angles under surface tractions. J Appl Mech 1971;38(2):377–86.
[32] Dempsey JP, Sinclair GB. On the singular behavior at the vertex of a bi-material wedge. J Elasticity 1981;11(3):317–27.
[33] Hein VL, Erdogan F. Stress singularities in a two-material wedge. Int J Fract Mech 1971;7(3):317–30.
[34] Gdoutos EE, Theocaris PS. Stress concentrations at the apex of a plane indenter acting on an elastic half-plane. J Appl Mech 1975;42(3):688–92.